

Date of publication xxxx 00, 0000, date of current version xxxx 00, 0000.

Digital Object Identifier 10.1109/ACCESS.2017.DOI

Vertical Wind Profile Characterization and Identification of Patterns based on a Shape Clustering Algorithm

A. MOLINA-GARCÍA¹, (IEEE Senior Member), A. FERNÁNDEZ-GUILLAMÓN¹, E. GÓMEZ-LÁZARO², (IEEE Senior Member), A. HONRUBIA-ESCRIBANO² AND MARÍA C. BUESO³.

¹Dept. of Electrical Engineering, Universidad Politécnica de Cartagena, 30202 Cartagena (Spain) (e-mail: angel.molina@upct.es; ana.fernandez@upct.es)

²Renewable Energy Research Inst. and DIEEAC-EDII-AB. Universidad de Castilla-La Mancha, 02071 Albacete (Spain) (e-mail: emilio.gomez@uclm.es; andres.honrubia@uclm.es)

³Dept. of Applied Mathematics and Statistics, Universidad Politécnica de Cartagena, 30202 Cartagena (Spain) (e-mail: mcarmen.bueso@upct.es)

Corresponding author: A. Molina-García (e-mail: angel.molina@upct.es).

This work was supported by the Spanish Ministry of the Economy and Competitiveness and the European Union —ENE2016-78214-C2-2-R— and by the Spanish Education, Culture and Sport Ministry —FPU16/04282—.

ABSTRACT Wind power plants are becoming a generally accepted resource in the generation mix of many utilities. At the same time, the size and the power rating of individual wind turbines have increased considerably. Under these circumstances, the sector is increasingly demanding an accurate characterization of vertical wind speed profiles to estimate properly the incoming wind speed at the rotor swept area and, consequently, assess the potential for a wind power plant site. The present paper describes a shape-based clustering characterization and visualization of real vertical wind speed data. The proposed solution allows us to identify the most likely vertical wind speed patterns for a specific location based on real wind speed measurements. Moreover, this clustering approach also provides characterization and classification of such vertical wind profiles. This solution is highly suitable for a large amount of data collected by remote sensing equipment, where wind speed values at different heights within the rotor swept area are available for subsequent analysis. The methodology is based on z -normalization, shape-based distance metric solution and the Ward-hierarchical clustering method. Real vertical wind speed profile data corresponding to a Spanish wind power plant and collected by using a commercial Windcube equipment during several months are used to assess the proposed characterization and clustering process, involving more than 100000 wind speed data values. All analyses have been implemented using open-source R -software. From the results, at least four different vertical wind speed patterns are identified to characterize properly over 90% of the collected wind speed data along the day. Therefore, alternative analytical function criteria should be subsequently proposed for vertical wind speed characterization purposes.

INDEX TERMS Clustering algorithms, Wind power generation, Patterns clustering

I. INTRODUCTION

MOST developed countries are now promoting large-scale integration of Renewable Energy Sources into power systems [1]. Among these renewables, wind power is considered the most efficient and developed energy source [2]. Indeed, it is expected that 323 GW of wind energy capacity will be installed in Europe by 2030, covering more than 30% of the electricity demand [3]. In fact, during recent decades, current wind turbine size has evolved from less than 100 kW to 3500 kW [4]. Full converter wind turbines can

provide greater flexibility and energy efficiency, converging power ratings between 4.5 MW and 7 MW [5]. At the same time, the increase in both the hub height and the area swept by the blades has drawn interest to better understanding the structure of the vertical profile of the horizontal wind [6]. Furthermore, since the power extracted by a wind turbine is highly dependent on the wind speed, an accurate estimation of vertical wind speed profiles v_H (the horizontal wind speed at height H) is required by the sector [7]. To determine the horizontal wind speed at hub height, two methods have

been widely used in the wind sector: (i) direct methods and (ii) indirect methods.

Direct methods are implemented by installing meteorological towers equipped with conventional wind speed meters at a suitable height or, more recently, by remote sensing such as SoDAR (Sonic Detection And Ranging) or LiDAR (Light Detection and Ranging) systems. The most commonly used speed meters are based on anemometers and windmills. Cup anemometers are formed by three or four cups equidistant from each other and coupled to a vertical rotational axis. Windmills are usually composed by four blades. Both anemometers and windmills have an error of around $\pm 2\%$, and collect horizontal wind speed values at only one height. Therefore, it should be required to estimate other wind speed values at the rotor swept area. SoDAR and LiDAR are based on the Doppler effect, receiving the reflection of sound and light, respectively. Apart from their significant accuracy (98% for SoDAR and 99.6% for LiDAR), they can collect wind speed data at different heights without needing a meteorological tower [8], which is an important advantage in comparison to the previous solutions. Moreover, LiDARs can also be used to obtain three-dimensional wind measurements [9]. Several studies can be found in the specific literature comparing these techniques or addressing different assessment analysis [10]. A comparison between LiDAR and cup anemometers was performed in [11], obtaining a high availability of 98% at the hub height in line with previous contributions [12]. A particular study in the Arctic middle atmosphere is described in [13], where mean wind speed values from LiDAR observations are compared to two different databases (ECMWF and HWM07). The results show that below $h \leq 55$ km the differences are smaller than 2 – 5 m/s. Recent contributions focused on optimizing LiDAR for wind turbine control can be found in [14], [15]. Regarding SoDAR solutions, suggested in [16], they can present root-mean-square errors of around 2% compared to mast-mounted cup anemometers. In [17], the results between SoDAR and the cup anemometer show some differences mainly due to the measurement field campaigns, which were conducted in different locations. A comparison between LiDAR, SoDAR and mast-mounted cup anemometer was carried out in [18]. Although a successful correlation level was found, both LiDAR and SoDAR collected lower wind speed values than the cup anemometers. According to [19], the SoDAR is highly dependent on temperature variation in the atmosphere, which is a substantial drawback compared to LiDAR solutions. However, a cost analysis reveals that SoDAR equipment is cheaper than the LiDAR [17].

Indirect wind speed estimation methods consist of measuring horizontal wind speed at a lower height and applying an extrapolation model to estimate the vertical wind speed profile. The most commonly used models are the power law, see (1), and the logarithmic law, see (2), [20].

$$v_H = v_{ref} \cdot \left(\frac{H}{H_{ref}} \right)^\alpha \quad (1)$$

$$v_H = \frac{u_*}{k} \cdot \ln \left(\frac{H}{z_0} \right), \quad (2)$$

where v_H is the horizontal wind speed at height H , v_{ref} the horizontal wind speed at the reference height H_{ref} , α the Hellmann's exponent depending on roughness of the underlying terrain, u_* the surface friction velocity, k the von Karman's constant and z_0 the surface roughness length. These approaches present substantial drawbacks, since parameters such as α and z_0 may vary significantly according to the year, month, hour of the day, or depending on wind direction and speed values. In this sense, [21] discusses the diurnal variation of α and the monthly variation of z_0 for three different locations in Italy. Recent empirical equations derived by applying the power law to the relationship between the increase of wind speed and fetch lengths at 1–5 km can be found in [22]. An alternative function is known as the Deaves and Harris model (D–H model), see (3). This solution proposes a more realistic and complex expression to consider the atmospheric boundary layer physics [23],

$$v_H = \frac{u_*}{k} \left[\ln \left(\frac{H}{z_0} \right) + 5.75 \left(\frac{H}{h} \right) - 1.88 \left(\frac{H}{h} \right)^2 - 1.33 \left(\frac{H}{h} \right)^3 + 0.25 \left(\frac{H}{h} \right)^4 \right] \quad (3)$$

$$h = \left(\frac{u_*}{B \cdot f} \right), \quad (4)$$

where v_H , u_* , k and z_0 are the same parameters as in (2), h is the equilibrium boundary layer height, determined from (4), f is the Coriolis parameter and $B = 6$ an empirical constant estimated from observed wind speed profiles [24].

A comparison between the D-H model and the power law based on real collected data is discussed in [25]. From the results, the authors affirm that the suitability of the selected model is highly dependent on atmospheric conditions: unstable, neutral or stable. A comparison between collected vertical wind speed profiles and these three indirect models was conducted in [26]. In this case, the averaged real wind speed profiles agree with the D-H and the logarithmic models below 200 and 100 m respectively. However, no similarities were found between the power law approach and the measured profiles. A similar study was performed in [27], where the D-H model provided the best estimations in comparison with measured data. Recently, new models have been proposed in the specific literature. In [28] a neuro-fuzzy model is provided to estimate vertical wind profiles up to 100 m by using measurements at 10, 20, 30 and 40 m. A method based on Wind Atlas Analysis and Application Program (WASP) to improve vertical wind speed estimations by least squares (LES) methodology is described in [29]. Two different proposals using artificial neural network are described in [30], estimating vertical wind speed values up to 100 m from measures at 10, 20 and 30 m. A time series model of wind speed for day ahead forecasting is developed in [31], based on linear and nonlinear autoregressive models

TABLE 1: Review of previous studies.

Ref.	Methodology used	Year
[13]	Comparison between LiDAR and two databases (ECMWF and HWM07)	2017
[17]	Comparison between SoDAR and cup anemometer	2017
[21]	Power law applied to anemometer measurements	2011
[25]	Comparison between D-H model and power law	2017
[32]	Revised power-law model	2018
[26]	Anemometers at different heights	2010
[27]	Comparison between LiDAR and data collected in a nearby place	2013
[28]	Adaptive neuro-fuzzy method	2011
[30]	Artificial neural network	2017
[33]	Comparison between power law, logarithmic law and real data	2015
[34]	Power law for low speed conditions (prevailing air and thermal pollution)	2017

with and without exogenous variables. A review of methodologies used in some of the previously mentioned studies is summarized in Table 1.

According to the specific literature, most contributions are thus focused on proposing different expressions to estimate vertical wind speed profiles from data provided by anemometers. Indeed, it is very common their application in the wind energy sector along the decades [35]–[37]. However, and assuming the power density (PD) —defined as the ratio between rated power output and rotor’s swept area (in W/m^2)— as a relevant indicator of the power wind turbine [38], several studies conclude that the wind speed at hub height is not representative for the whole area. Moreover, it leads to inconsistencies in power curve measurements for large wind turbine [39]. For this reason, recent works affirm that it is preferable to take measures at two or three levels, for one period at least six months [40]. Post processing methods should be then applied on these collected raw data to extract explanatory information of most likely vertical wind speed profiles. Under this scenario, there is a lack of contributions devoted to characterizing a large amount of real wind speed data. Moreover, solutions to identify common vertical wind speed patterns and, consequently, make both representation and characterization easier are more and more required by the sector to analyze a location and the corresponding vertical wind resource in detail. Therefore, a characterization of raw wind power data is needed to estimate properly the wind power capable to produce energy and subsequently to allow us new proposals of vertical wind speed profile modeling, since nowadays there is no uniform analytic expression valid for all wind stability conditions [41]. The main contributions of this paper are then summarized as follows:

- A novel wind speed analysis to identify vertical wind speed patterns from a large amount of collected wind speed data is proposed and assessed.
- A shape-based clustering analysis is evaluated to provide most likely vertical wind speed patterns along the day based on real wind speed data collected with a LiDAR system.
- The proposed solution, implemented in the open-source

R-software with unrelevant computational time cost, can be adapted to different locations from the corresponding raw data and the field-measurement campaigns.

This work is in line with previous contributions by the authors, where the aggregated wind power generation was characterized based on Weibull mixtures [42]. The rest of the paper is organized as follows: Section II discusses the time-series clustering techniques used to characterize wind speed profiles; Section III describes the proposed methodology; the results are described and discussed in Section IV; and, finally, the conclusions are presented in Section V.

II. FUNCTIONAL CLUSTERING: BACKGROUND AND RELATED WORK

A. GENERAL OVERVIEW

Clustering is one of the most commonly used data mining techniques to find homogeneous subgroups of entities depicted in a set of data [43], [44]. A cluster analysis involves sorting data objects into groupings (labeled as clusters) based on similarity [45]. Although the notion of ‘cluster’ is not unique [46], the global goal is that the objects of a group are similar to one another and different from the ones in other groups [47]. According to [48], various clustering algorithms can be found in the specific literature:

- Hierarchical methods: Clusters are determined by recursively partitioning the instances. There are two types: agglomerative hierarchical clustering (objects are considered as clusters that are merged successively) and divisive hierarchical clustering (all objects belong to one cluster that is divided successively into sub-clusters).
- Partitioning methods: The objects are relocated by moving them from one cluster to another, starting from an initial partitioning. There are two methods: error minimization algorithms —these find a clustering structure that minimizes a certain error criterion. This measures the ‘distance’ of each object to its representative value— and graph-theoretic clustering —determining clusters via graphs—.
- Density-based methods: It is assumed that the points that belong to each cluster are drawn from a specific probability distribution.
- Model-based clustering methods: Optimizing the fit between given data and some mathematical models.

A large number of functional clustering applications can be found in the literature review [49], mainly focused on life sciences [50]. Nevertheless, a number of authors have proposed the use of functional clustering approaches for power system purposes. A comparison of various unsupervised clustering algorithms to group customers with similar electrical behavior is provided in [51]. In [52], a functional clustering procedure is used to classify the daily power load curves of four separated periods, providing a short-term peak load forecasting methodology. A clustering methodology able to improve short-term functional time series forecasts

of household-level electricity demand is presented in [53]. A forecasting model for day-ahead and hour-ahead load predictions is developed in [54] based on artificial neural networks and clustering. A novel clustering-based fuzzy wavelet neural network model is also proposed in [55]. Data mining techniques have been also proposed to analyze SCADA measurements collected on onshore wind power plants, but focused on power curve analysis [56]. In our specific study, and taking into account the efficiency issue of hierarchical clustering, which can be applied to most types of data [57], the agglomerative hierarchical clustering is selected. This approach usually involves higher computational time costs than partitional clustering, but requires non-predefined parameters [58]. Specifically, Ward's hierarchical clustering method is used to estimate the different clusters, which is carried out in a multivariate Euclidean space [59].

B. DISSIMILARITY MEASURES

With regard the time-series clustering, different algorithms have been developed in the specific literature considering a wide set of dissimilarity or distance measures [60]. One of the most popular and field-tested similarity measures is the Dynamic Time Warping (DTW) distance, based on the optimum warping path between time-series [61]. DTW has been widely used in many areas and is a popular automatic speech recognition (ASR) method [62]. Indeed, it is a flexible and much more robust distance measure, allowing similar shapes to be matched even if they are out of the phase in the time axis [63]. Given two discrete time-series $X = (x_1, x_2, \dots, x_n)$ and $Y = (y_1, y_2, \dots, y_m)$ with $n, m \in \mathbb{N}$, we define the cross-distance matrix ($M \in \mathbb{R}^{n,m}$) as follows:

$$m_{ij} = d(i, j) = f(x_i, y_j) \geq 0. \quad (5)$$

The most common choice is to assume the Euclidean distance $m_{ij} = d(i, j) = (x_i - y_j)^2$. The algorithm then finds the alignment path through the low-cost areas of the cross-distance matrix. It is typically subjected to the following constraints: boundary conditions, continuity and monotonicity [64]. A warping path that minimizes the distance between both time-series can then be estimated by [65]:

$$DTW(X, Y) = \min \left[\sum_{k=1}^K m_{kk} = d(k, k) = f(x_k, y_k) \right], \quad (6)$$

where $\max(n, m) \leq K \leq m + n + 1$. Further information and some examples of DTW technique can be found in [66]–[68]. In addition, Fig. 1 shows an example of the DTW technique application and a comparison to the Euclidean distance approach for two random trajectories. The *dtw*-function is applied by using the *dtw* R-software package [69].

DTW approach can also be extended to measure the similarity between two N -dimensional sequences [70]. An example of a multi-dimensional Dynamic Time Warping (msDTW) approach can be found in [71]. According to some authors, and assuming that DTW is a major solution in the

field of time series classification problem, it has quadratic space and time complexity that might lead to memory problems under long time series data [72]. As a faster alternative to the DTW algorithm, the Shape-Based Distance (SBD) metric was proposed by [73]. It is based on coefficient-normalized cross-correlation. It is used in the present work as an improved methodology of DTW metric solutions. To provide scale invariance and remove inherent distortion in the collected data, we implement the z -normalization of the horizontal wind speed values. This z -normalization is based on the standard $(0, 1)$ statistical normalization: vectors are linearly transformed by subtracting their feature means and dividing by their standard-deviations [74],

$$z_i = \frac{x_i - \mu_X}{\sigma_X}, \quad (7)$$

All analyses have been conducted using open-source R-software [75]. The *dtwclust* R-package is used for the SBD metric estimation [76].

III. METHODOLOGY

Taking into account both the SBD algorithm and Ward's hierarchical clustering method previously discussed in Section II, a characterization methodology to identify wind speed profile patterns and visualize most common tendencies is now described in detail. This approach allows us to characterize large amounts of wind speed data collected in real locations by means of clustering and pattern identification. The solution is thus highly suitable for data collected by remote sensing equipment, where wind speed values at different heights are available to be analyzed. Fig. 2 shows schematically the data structure and an example of horizontal wind speed data for the different heights and by considering a specific day (Day_i) and hour (Hour_k).

The proposed methodology is firstly based on a filtering real data stage. With this aim, a preliminary data analysis was carried out to remove non-expected and/or wrong data. Subsequently, wind speed curves with missing data or more than 50% of the wind speed values below 4 m/s were not considered. Most wind turbines currently have a minimum starting wind speed range over 4 m/s. Recent contributions focused on dynamic data filtering for LiDAR wind speed measurements can be found in [77]. After this initial filtering process, and based on previous studies from collected data on on-shore Spanish wind power plants, it was detected that some of the $v - H$ curves were discordant. Indeed, it was even found that some of them were not functions at all, having two or more H values for just one v . To solve this problem, the author propose an axis rotation. $H - v$ curves are thus obtained, solving aforementioned the problem. It is worth noting that this drawback, mainly related to real data collected at different heights in on-shore wind power plants, has not been widely discussed in the specific literature, being neglected by most previous contributions. The filtered wind speed data are then fulfilled by using the aspline function with the objective of defining a unique and homogeneous

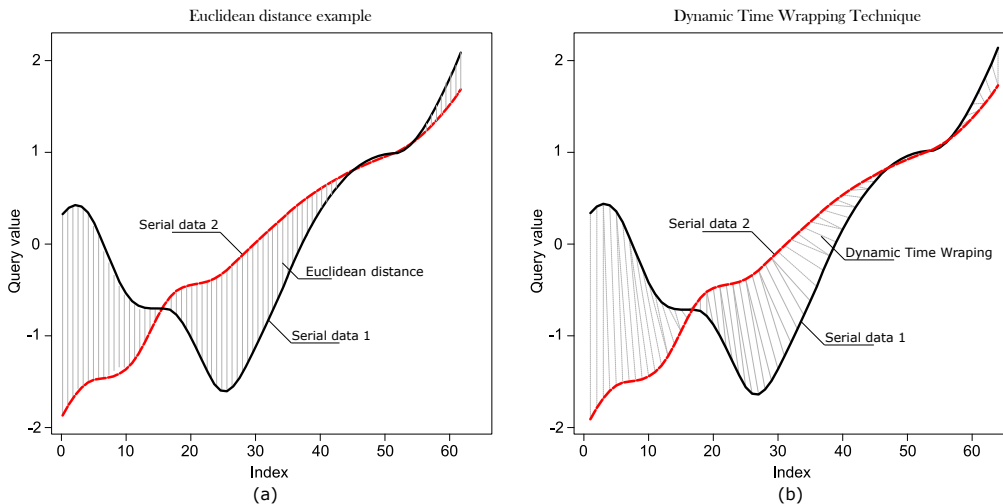


FIGURE 1: Dynamic Time Wrapping (DTW) technique example.

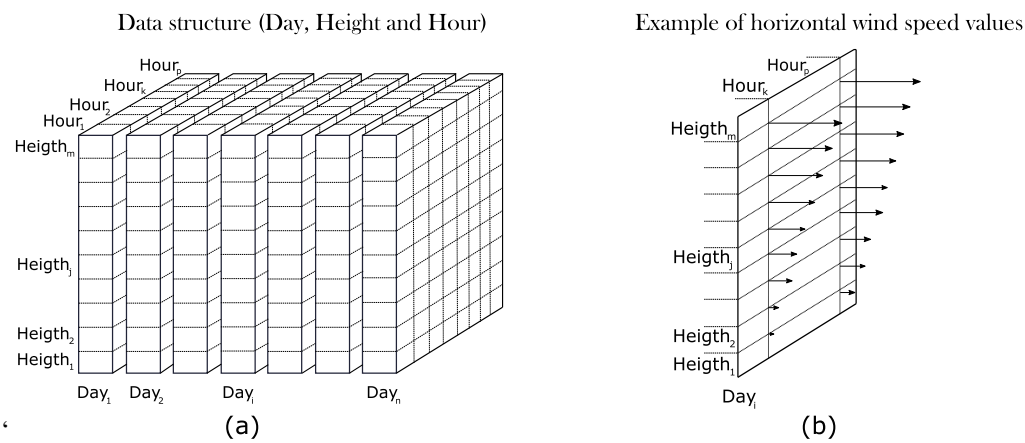


FIGURE 2: General data scheme and example of horizontal wind speed data. General overview

height interval: from 40 to 160 m. Fig. 3 shows examples of wind speed collected data and their corresponding filtered and fulfilled values by the aspline function. Real data were collected for three months at a Spanish wind power plant located in the southeast of Spain. The wind speed data collected at different hours are summarized in the figure.

From these homogeneous groups of wind speed profiles, an interpolation process is then applied on a common grid, providing a positive power length of 2. In our case, a total of 512 points are estimated, being a 2 potential (2^9). The Akima R-software package is used for this interpolation process. Further information about this package can be found in [78]. Fig. 4 describes schematically the proposed axis rotational and spline process and the corresponding interpolated vertical wind speed profiles.

As was previously discussed in Section II, and aiming to provide scale invariance and remove inherent distortion in the data, a z -normalization process is applied to the spline values. Each wind speed curve is linearly transformed by subtracting their feature means and dividing by their standard-deviations. Fig. 5 shows an example of z -normalization process from real

wind speed data previously filtered and splined. The SBD metric is then applied on the z -normalized data, providing an estimation of distances between the wind speed curves. These curves are divided into different hours of the day and, subsequently, distances among these curves correspond to those curves collected within the same hour. Finally, Ward's hierarchical clustering method was applied to estimate the most likely wind speed profile patterns for each time interval. Fig. 6 describes schematically the wind speed data structure and the selection process for a specific hour ($Hour_k$). The clustering application usually involves a visual inspection of the clustering in terms of deciding the optimal number of clusters. Other approaches propose different decision criteria for the optimal cluster number [79]. In our opinion, this optimal number of clusters is outside the scope of the present contribution and subsequently, the optimal number of clusters is then considered as a user-decision. From the corresponding wind speed patterns, a suitable and summarized visualization of a large amount of real collected data through a reduced number of profiles is then provided. Indeed, these wind speed patterns give an accurate and precise prelimi-

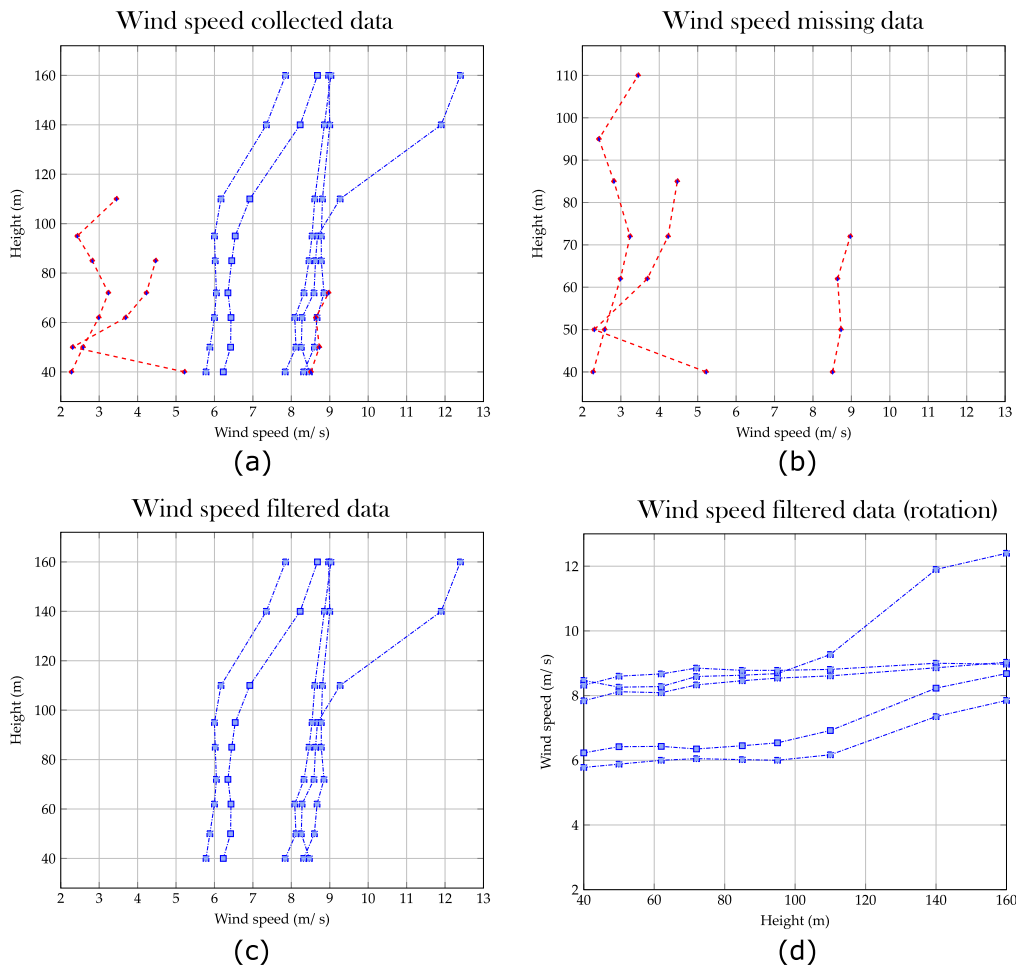


FIGURE 3: Example of filtering process application (Spanish Wind Power Plant).

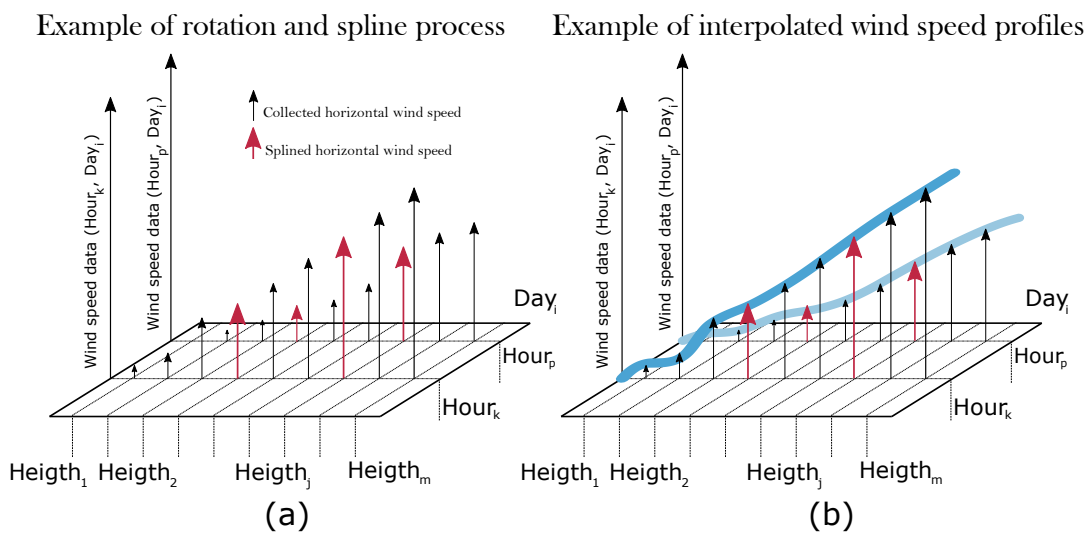


FIGURE 4: Axis rotational, spline data process and interpolated vertical wind speed profiles. General overview

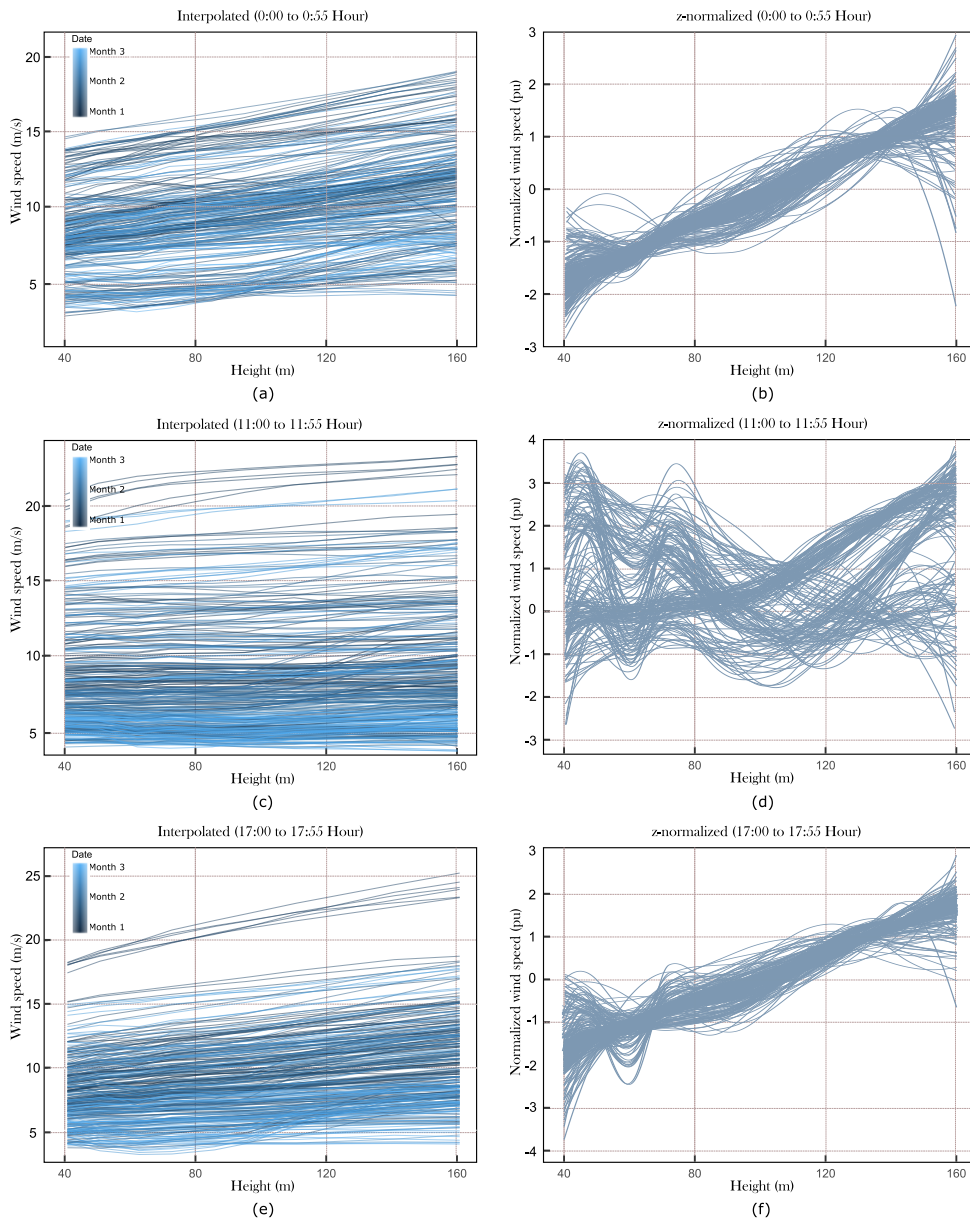


FIGURE 5: Example of interpolation and z -normalization process (Spanish Wind Power Plant).

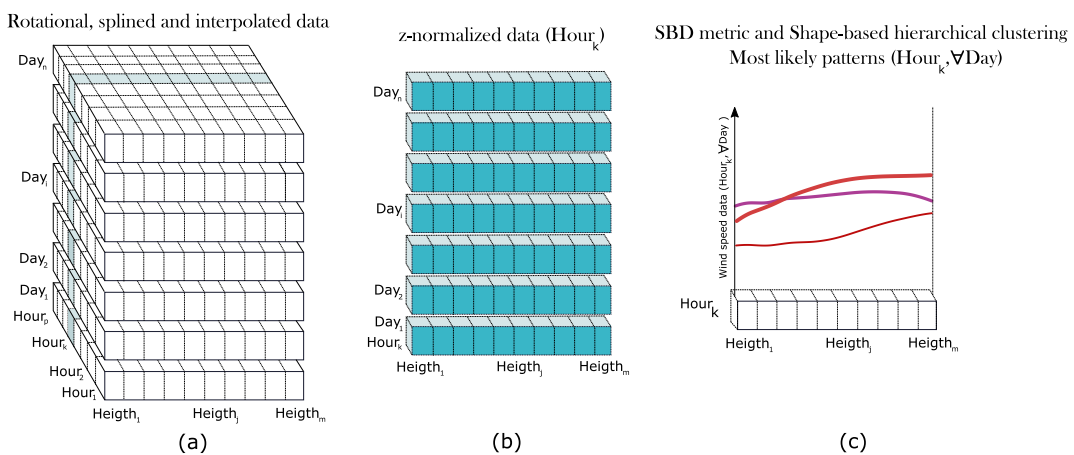


FIGURE 6: z -normalized, SBD metric and clustering process. General overview

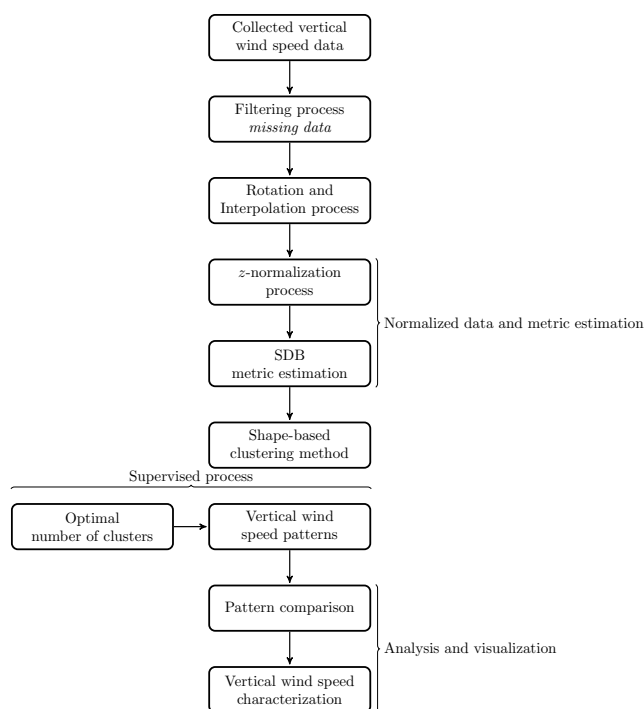


FIGURE 7: Proposed clustering and analysis methodology.



FIGURE 8: WindCurbe LiDAR equipment: example of field-test campaign (Albacete, Spain).

nary analysis about the possibilities of proposing different analytical functions to characterize real wind speed curves. Moreover, the proposed visualization and characterization solution of real data also provides additional information to study collected data in detail and characterize the available wind resource. Fig. 7 summarizes the methodology proposed in this work.

IV. RESULTS

A. PRELIMINARIES

Wind speed data were collected at two Spanish wind power plants connected to the grid and located in the south of Spain. Different field measurement campaigns were carried out by using LiDAR equipment. More specifically, a commercial WindCube was installed in these locations to collect wind speed data over three months. Fig. 8 shows the equipment used for the field measurement campaigns. Wind speed curves were measured and collected with a 10 minute sample time interval. The height range of measurements was from 40 m to 200 m. Nevertheless, and with the aim of maximizing the number of data used for clustering purposes, wind speed heights were limited from 40 to 160 m since a significant amount of data at 200 m corresponded to wrong values or not-a-number values, as was mentioned in Section III. A total amount of 110230 data were initially analysed. After the filtering process, a total wind speed values of 61551 were selected, corresponding to 6839 vertical wind speed profiles. By considering this initial group of vertical wind speed values, a subsequent characterization process is thus required by the sector to visualize the most likely vertical

wind speed patterns.

Fig. 9 shows an example of the wind speed variability for a specific wind power plant and location, taking into account both maximum and minimum wind speed values based on the collected data at different heights —40, 52, 62, 72, 85, 95, 110, 140 and 160 m—. As can be seen, there are relevant oscillations within the same hour for each day. Wind speed data are then z -normalized to estimate their corresponding wind speed curve patterns for each hour. Subsequently, a clustering process is applied on each hour to determine the most likely patterns throughout the day for the different hours.

B. FUNCTIONAL CLUSTERING CHARACTERIZATION. ANALYSIS

From the z -normalized wind speed data, and after dividing into different hours throughout the day, the SBD metric solution was applied to determine distances between splined vertical wind speed curves. According to the proposed methodology and as was previously discussed, the Ward's hierarchical clustering method involves a visual inspection of the results to determine a suitable number of clusters. Note that hierarchical clustering results are graphically represented on dendrograms. Fig. 10 depicts some dendrogram examples for different hours. Under these results, the number of 9 clusters was selected since it was considered suitable by the authors in order to characterize vertical wind speed profile variability across the different hours. Further information about a semi-supervised hierarchical clustering framework based on ultrametric dendrogram distance can be found in [80].

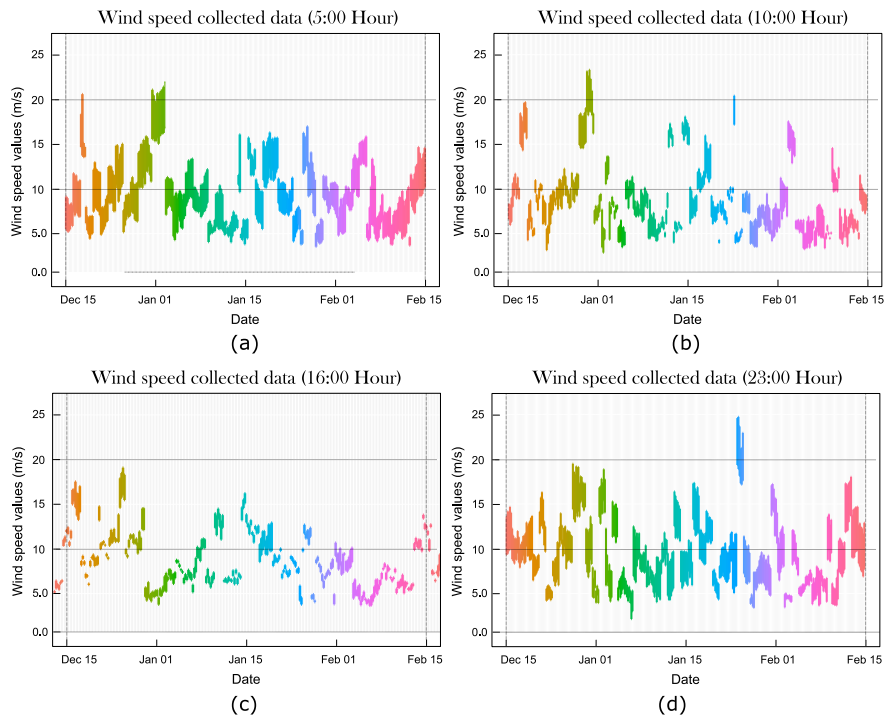


FIGURE 9: Example of wind speed data for a field measurement campaign (Collected data at different hours, Wind power plant located in Albacete, Spain).

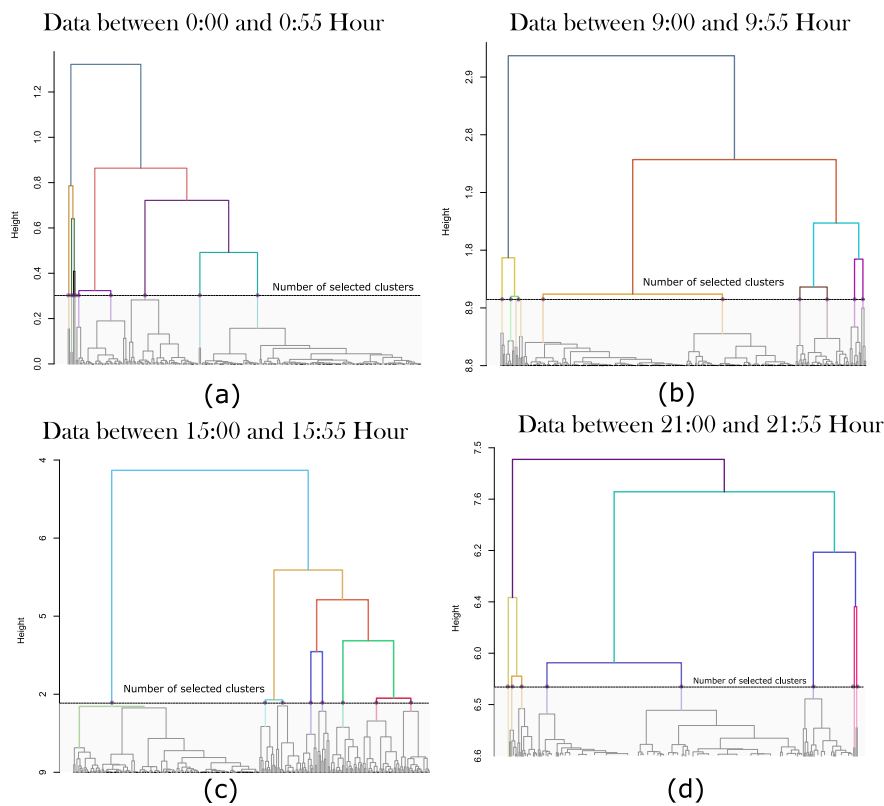


FIGURE 10: An illustrative examples of hierarchical clustering dendrograms.

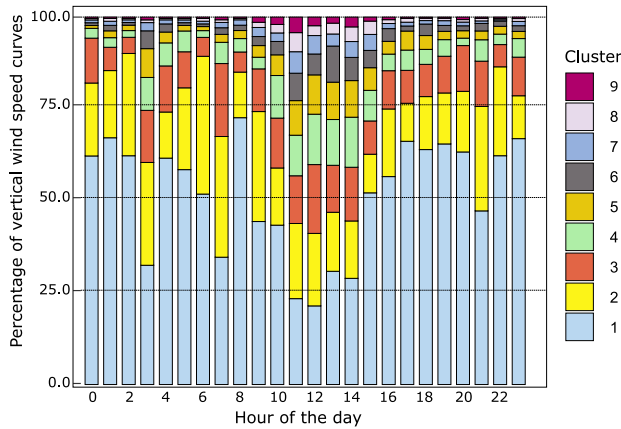


FIGURE 11: Cluster distribution per hours. Ward’s hierarchical clustering process.

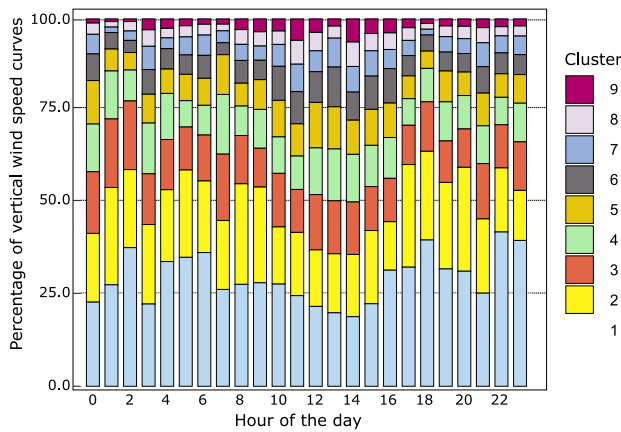


FIGURE 12: Cluster distribution per hours. Partitional clustering process.

Assuming a number of 9 clusters as a suitable classification of the different vertical wind speed groups for each hour, Fig. 11 summarizes the percentage of each cluster according to the hour of the day. As can be seen, night-time hours can be characterized by a lower amount of clusters in comparison to daylight hours. Indeed, 3 clusters accounts for over 75% of the vertical wind speed profiles for the night-time hours. However, daylight hours require a higher number of clusters to be characterized properly. As an example, 5 clusters are needed to account for 75% of the vertical wind speed data between 12:00 and 12:55 Hour. This results are in line with other clustering techniques, such as partitional process. Aiming to compare both approaches Fig. 12 shows the percentages for each hour when partitional clustering process is applied on the collected data. According to both methodologies, different vertical wind speed patterns are thus required to characterize the collected data, presenting a relevant heterogeneity in the vertical wind speed profiles. The rest of analysis is conducted according to the Ward’s hierarchical clustering results, by considering the percentage of clusters summarize in Fig. 11.

Fig. 13 summarizes the classification of the collected vertical wind speed profiles according to the different clusters for data gathered between 4:00 and 4:55 hour. In addition, the vertical wind speed patterns are also included in the figure, as well as the percentage of data corresponding to each cluster by considering the percentage of clusters for each hour depicted in Fig. 11. From these results, the proposed characterization process allows us to identify the most likely vertical wind speed patterns by considering the gathered data in a specific location and attending to the different hours. Moreover, a comparison between the vertical wind speed patterns for different hours are also available from these results. With this aim, Fig. 14 compares the most representative vertical wind speed patterns for different hours. In this case, these results include vertical wind speed patterns representing around 90% of the collected wind speed data for the different hours —percentages included in the legend—, and based on the percentages depicted in Fig. 11. As can be seen, these averaged vertical wind speed patterns differ significantly among them, and thus, a relevant loss of information —in terms of vertical wind speed profiles and wind resource estimation— would be then assumed if these patterns were reduced to only one representative wind speed curve. This is a relevant contribution of the paper, being thus required an alternative set of analytical functions to characterize real vertical wind speed data for different hours and locations. Under these assumptions, some extrapolation model functions are thus required to represent the collected wind speed profiles in an accurate and suitable way. This analysis is in line with the indirect method discussed in Section I. Nevertheless, it is outside the scope of the present work, but is currently one of the authors’ fields of interest.

As an additional contribution of the paper, and in order to reduce significantly the data to be stored, the authors propose saving the most representative patterns for each hour. Consequently, only means, standard-deviations and the corresponding cluster from the collected vertical wind speed data are stored. From this reduced information, it is possible to estimate any vertical wind speed $v - H$ data for a specific hour of the day and location. Aiming to validate this additional proposal, Fig. 15 compares the estimated and collected wind speed $v - H$ profiles for the most representative clusters between 15:00 and 15:55 hour. This figure also includes correlation frequency histogram graphs, as a measure of estimation accuracy. By considering the frequency histogram graphs, the estimated $v - H$ wind speed profiles are very close to their corresponding real collected data. Therefore, the vertical wind speed clustering patterns are able to represent not only the most representative wind speed data, but also the collected $v - H$ wind speed profiles. This additional proposal allows the stored data to be significantly reduced after intensive field-test campaign measurements. Moreover, it allows a more comprehensive data structure, since each of the most representative patterns can be stored with its corresponding means and standard-deviation values, providing a direct estimation of the $v - H$ wind speed data.

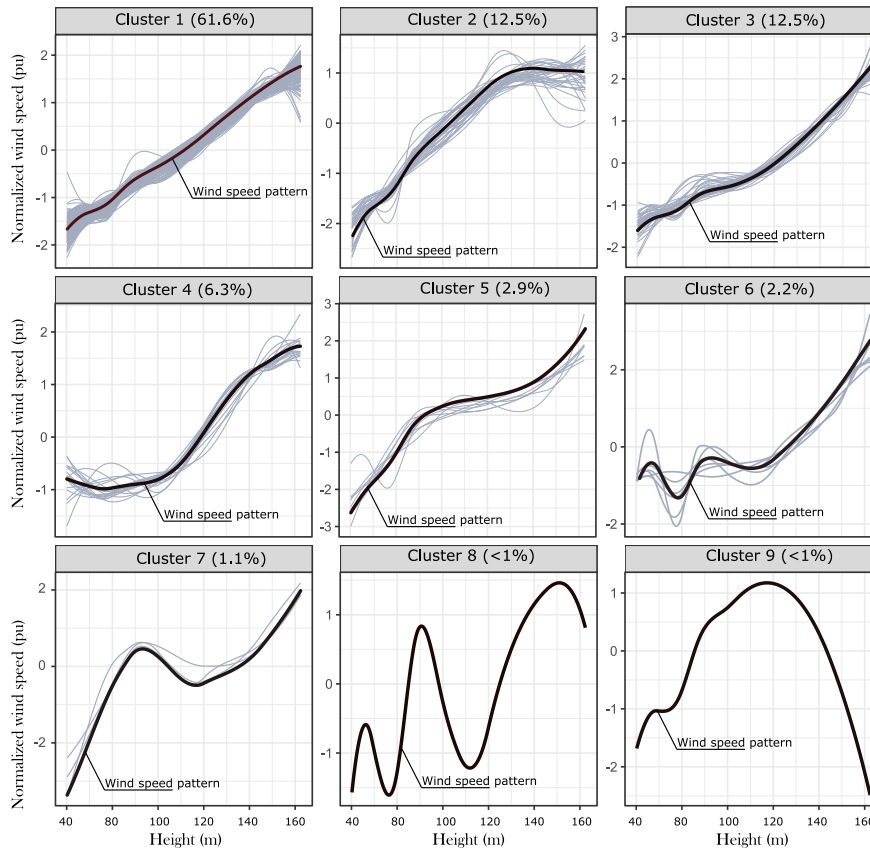


FIGURE 13: Example of z -normalized vertical wind speed distributed profiles (from 4:00 to 4:55 Hour). Ward's hierarchical clustering process.

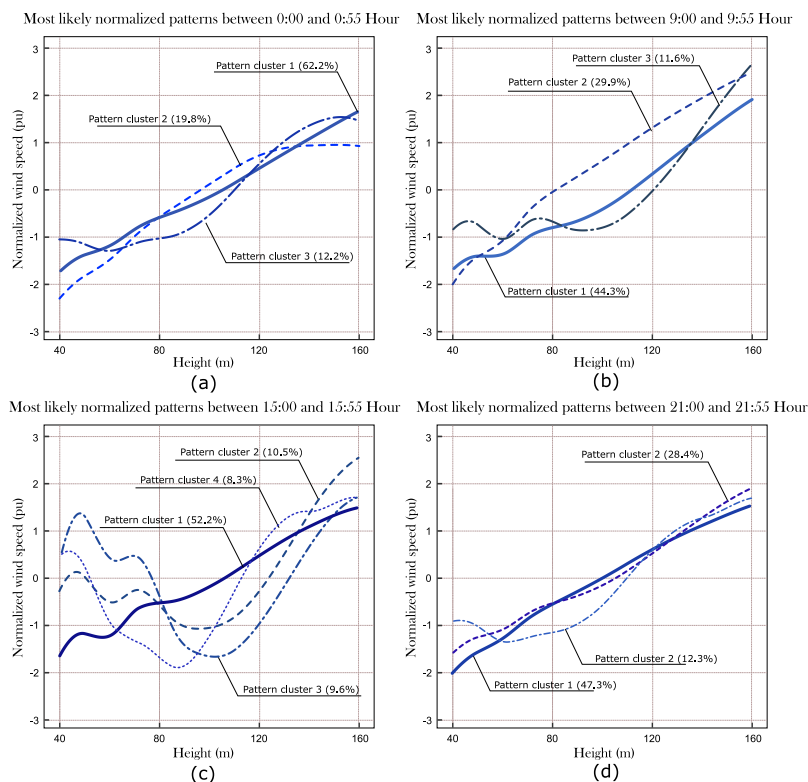


FIGURE 14: Examples of the most likely vertical wind speed normalized patterns. Results corresponding to several hours.

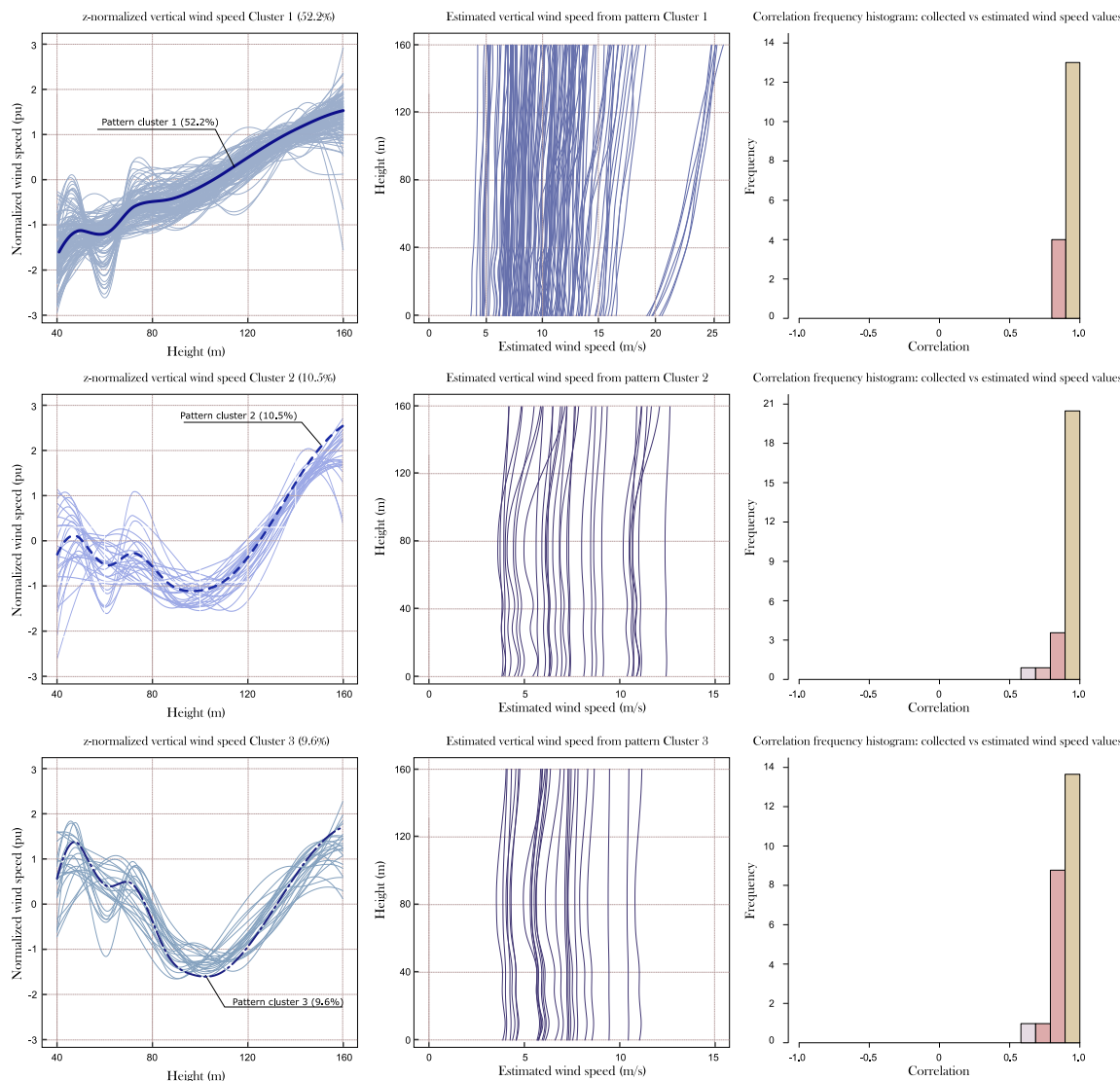


FIGURE 15: Example of estimated vs collected vertical wind speed data (Most representative clusters between 15:00 and 15:55 Hour)

V. CONCLUSION

A novel methodology to estimate vertical wind speed patterns from collected wind speed data is described and assessed. The proposed methodology uses a Shape-Based Distance metric to characterize wind speed similarity groups. A Ward hierarchical clustering method is applied to determine the most likely vertical wind speed patterns at each hour for a specific location. The proposed solution is assessed through real wind speed data collected with a LiDAR system over three months at a Spanish wind power plant, accounting for more than 100000 wind speed values. A preliminary filtered and homogenized process is proposed to provide scale invariance and remove inherent distortion in the initial data. From the results, at least four different vertical wind speed patterns are needed to characterize over 90% of the 6839 collected and filtered vertical wind speed profiles. Moreover, significant differences among patterns are found and subsequently, new

analytical function criteria should be proposed as vertical wind speed value extrapolation models. All analyses were implemented using open-source *R*-software. The *R* code is available from the authors upon request. Further analysis of alternative extrapolation model functions to characterize in detail the incoming wind speed at the rotor swept area is currently a relevant topic for future works.

ACKNOWLEDGMENT

The authors are grateful for the financial support from the Spanish Ministry of the Economy and Competitiveness and the European Union —ENE2016-78214-C2-2-R— and the Spanish Education, Culture and Sport Ministry —FPU16/04282—.

REFERENCES

- [1] S. Tselepis and J. Nikolettatos, "Renewable energy integration in power grids," 04 2015.
- [2] A. Thakur, S. Panigrahi, R. Behera et al., "A review on wind energy conversion system and enabling technology," in *Electrical Power and Energy Systems (ICEPES)*, International Conference on. IEEE, 2016, pp. 527–532.
- [3] "Wind energy in europe: Scenarios for 2030," *Wind Europe*, 2017.
- [4] G. J. Herbert, S. Iniyar, E. Sreevalsan, and S. Rajapandian, "A review of wind energy technologies," *Renewable and Sustainable Energy Reviews*, vol. 11, no. 6, pp. 1117–1145, 2007.
- [5] J. Jallad, S. Mekhilef, and H. Mokhlis, "Frequency regulation strategies in grid integrated offshore wind turbines via vsc-hvdc technology: A review," *Energies*, vol. 10, no. 9, p. 1244, 2017.
- [6] S.-E. Gryning, R. Floors, A. Peña, E. Batchvarova, and B. Brümmner, "Weibull wind-speed distribution parameters derived from a combination of wind-lidar and tall-mast measurements over land, coastal and marine sites," *Boundary-Layer Meteorology*, vol. 159, no. 2, pp. 329–348, 2016.
- [7] F. Bañuelos-Ruedas, C. Angeles-Camacho, and S. Rios-Marcuello, "Analysis and validation of the methodology used in the extrapolation of wind speed data at different heights," *Renewable and Sustainable Energy Reviews*, vol. 14, no. 8, pp. 2383–2391, 2010.
- [8] A. Honrubia-Escribano, E. Gómez-Lázaro, Á. Molina-García, and A. Viguera-Rodríguez, "Wind resource assessment systems: Review of new solutions based on laser technology," *DYNA-Ingeniería e Industria*, vol. 87, no. 5, 2012.
- [9] P. Doubrawa, R. J. Barthelmie, H. Wang, S. C. Pryor, and M. J. Churchfield, "Wind turbine wake characterization from temporally disjunct 3-d measurements," *Remote Sensing*, vol. 8, no. 11, p. 939, 2016.
- [10] R. Bos, A. Giyanani, and W. Bierbooms, "Assessing the severity of wind gusts with lidar," *Remote Sensing*, vol. 8, no. 9, p. 758, 2016.
- [11] A. Westerhellweg, B. Canadillas, A. Beeken, and T. Neumann, "One year of lidar measurements at fino1-platform: Comparison and verification to met-mast data," in *Proceedings of 10th German wind energy conference DEWEK*, 2010, pp. 1–5.
- [12] M. Post, R. Schwiesow, R. Cupp, D. Haugen, and J. Newman, "A comparison of anemometer-and lidar-sensed wind velocity data," *Journal of Applied Meteorology*, vol. 17, no. 8, pp. 1179–1181, 1978.
- [13] J. Hildebrand, G. Baumgarten, J. Fiedler, and F.-J. Lübken, "Winds and temperatures of the arctic middle atmosphere during january measured by doppler lidar," *Atmospheric Chemistry and Physics*, vol. 17, no. 21, pp. 13 345–13 359, 2017.
- [14] E. Simley, H. First, F. Haizmann, and D. Schlipf, "Optimizing lidars for wind turbine control applications. results from the iea wind task 32 workshop," *Remote Sensing*, vol. 10, no. 6, 2018.
- [15] A. Clifton, P. Clive, J. Gottschall, D. Schlipf, E. Simley, L. Simmons, D. Stein, D. Trabucchi, N. Vasiljevic, and I. Würth, "Iea wind task 32: Wind lidar identifying and mitigating barriers to the adoption of wind lidar," *Remote Sensing*, vol. 10, no. 3, p. 406, 2018.
- [16] S. Bradley, "Aspects of the correlation between sodar and mast instrument winds," *Journal of Atmospheric and Oceanic Technology*, vol. 30, no. 10, pp. 2241–2247, 2013.
- [17] K. S. Khan and M. Tariq, "Wind resource assessment using sodar and meteorological mast—a case study of pakistan," *Renewable and Sustainable Energy Reviews*, 2017.
- [18] S. Lang and E. McKeogh, "Lidar and sodar measurements of wind speed and direction in upland terrain for wind energy purposes," *Remote Sensing*, vol. 3, no. 9, pp. 1871–1901, 2011.
- [19] C. B. Hasager, A. Pena, M. B. Christiansen, P. Astrup, M. Nielsen, F. Monaldo, D. Thompson, and P. Nielsen, "Remote sensing observation used in offshore wind energy," *IEEE Journal of Selected Topics in Applied Earth Observations and Remote Sensing*, vol. 1, no. 1, pp. 67–79, March 2008.
- [20] Y. Liu, D. Chen, Q. Yi, and S. Li, "Wind profiles and wave spectra for potential wind farms in south china sea. part i: Wind speed profile model," *Energies*, vol. 10, no. 1, p. 125, 2017.
- [21] G. Gualtieri and S. Secci, "Wind shear coefficients, roughness length and energy yield over coastal locations in southern italy," *Renewable Energy*, vol. 36, no. 3, pp. 1081–1094, 2011.
- [22] S. Shimada, Y. Takeyama, T. Kogaki, T. Ohsawa, and S. Nakamura, "Investigation of the fetch effect using onshore and offshore vertical lidar devices," vol. 10, pp. 1–14, September 2018.
- [23] Q. Li, L. Zhi, and F. Hu, "Field monitoring of boundary layer wind characteristics in urban area," *Wind and Structures*, vol. 12, no. 6, p. 553, 2009.
- [24] H. W. Tieleman, "Strong wind observations in the atmospheric surface layer," *Journal of Wind Engineering and Industrial Aerodynamics*, vol. 96, no. 1, pp. 41 – 77, 2008.
- [25] G. Gualtieri, "Wind resource extrapolating tools for modern multi-mw wind turbines: Comparison of the deaves and harris model vs. the power law," *Journal of Wind Engineering and Industrial Aerodynamics*, vol. 170, pp. 107–117, 2017.
- [26] Q. Li, L. Zhi, and F. Hu, "Boundary layer wind structure from observations on a 325 m tower," *Journal of wind engineering and industrial aerodynamics*, vol. 98, no. 12, pp. 818–832, 2010.
- [27] D. R. Drew, J. F. Barlow, and S. E. Lane, "Observations of wind speed profiles over greater london, uk, using a doppler lidar," *Journal of Wind Engineering and Industrial Aerodynamics*, vol. 121, pp. 98–105, 2013.
- [28] M. Mohandes, S. Rehman, and S. Rahman, "Estimation of wind speed profile using adaptive neuro-fuzzy inference system (anfis)," *Applied Energy*, vol. 88, no. 11, pp. 4024–4032, 2011.
- [29] Z. Durisić and J. Mikulović, "A model for vertical wind speed data extrapolation for improving wind resource assessment using wasp," *Renewable Energy*, vol. 41, pp. 407 – 411, 2012. [Online]. Available: <http://www.sciencedirect.com/science/article/pii/S0960148111006185>
- [30] M. S. Islam, M. Mohandes, and S. Rehman, "Vertical extrapolation of wind speed using artificial neural network hybrid system," *Neural Computing and Applications*, vol. 28, no. 8, pp. 2351–2361, 2017.
- [31] M. Lydia, S. S. Kumar, A. I. Selvakumar, and G. E. P. Kumar, "Wind resource estimation using wind speed and power curve models," *Renewable Energy*, vol. 83, pp. 425–434, 2015.
- [32] Y. Liu, D. Chen, S. Li, and P. Chan, "Revised power-law model to estimate the vertical variations of extreme wind speeds in china coastal regions," *Journal of Wind Engineering and Industrial Aerodynamics*, vol. 173, pp. 227–240, February 2018.
- [33] F. A. Hadi, "Diagnosis of the best method for wind speed extrapolation," *International Journal of Advanced Research in Electrical, Electronics and Instrumentation Engineering*, vol. 4, no. 10, 2015.
- [34] H. Kikumoto, R. Ooka, H. Sugawara, and J. Lim, "Observational study of power-law approximation of wind profiles within an urban boundary layer for various wind conditions," *Journal of Wind Engineering and Industrial Aerodynamics*, vol. 164, pp. 13–21, 2017.
- [35] S. Pindado, J. Cubas, and F. Sorribes, "The cup anemometer, a fundamental meteorological instrument for the wind energy industry. research at the IDR/UPM institute," *Sensors (Basel, Switzerland)*, vol. 14, pp. 21 418–21 452, June 2014.
- [36] P. Pinson and J. W. Messner, "Chapter 9 - application of postprocessing for renewable energy," in *Statistical Postprocessing of Ensemble Forecasts*, S. Vannitsem, D. S. Wilks, and J. W. Messner, Eds. Elsevier, 2018, pp. 241 – 266. [Online]. Available: <http://www.sciencedirect.com/science/article/pii/B9780128123720000091>
- [37] A. T. Abolude and W. Zhou, "A comparative computational fluid dynamic study on the effects of terrain type on hub-height wind aerodynamic properties," *Energies*, vol. 12, no. 1, 2018. [Online]. Available: <http://www.mdpi.com/1996-1073/12/1/83>
- [38] I. Arrambide, I. Zubia, and A. Madariaga, "Critical review of offshore wind turbine energy production and site potential assessment," *Electric Power Systems Research*, vol. 167, pp. 39 – 47, 2019. [Online]. Available: <http://www.sciencedirect.com/science/article/pii/S0378779618303341>
- [39] R. Wagner, M. Courtney, J. Gottschall, and P. Lindelöw-Marsden, "Accounting for the speed shear in wind turbine power performance measurement," *Wind Energy*, vol. 14, no. 8, pp. 993–1004, 2011.
- [40] M. Elamouri, F. B. Amar, and A. Trabelsi, "Vertical characterization of the wind mode and its effect on the wind farm profitability of sidi daoud – tunisia," *Energy Conversion and Management*, vol. 52, no. 2, pp. 1539 – 1549, 2011. [Online]. Available: <http://www.sciencedirect.com/science/article/pii/S0196890410004589>
- [41] G. Gualtieri and S. Secci, "Methods to extrapolate wind resource to the turbine hub height based on power law: A 1-h wind speed vs. weibull distribution extrapolation comparison," *Renewable Energy*, vol. 43, pp. 183–200, 2012. [Online]. Available: <http://www.sciencedirect.com/science/article/pii/S0960148112000109>
- [42] E. Gómez-Lázaro, M. C. Bueso, M. Kessler, S. Martín-Martínez, J. Zhang, B.-M. Hodge, and A. Molina-García, "Probability density function characterization for aggregated large-scale wind power based on weibull mixtures," *Energies*, vol. 9, no. 2, 2016.

- [43] A. Antoniadis, X. Brossat, J. Cugliari, and J.-M. Poggi, "Clustering functional data using wavelets," *International Journal of Wavelets, Multiresolution and Information Processing*, vol. 11, no. 01, p. 1350003, 2013.
- [44] T. Tarpey and K. K. Kinader, "Clustering functional data," *Journal of Classification*, vol. 20, no. 1, pp. 093–114, 2003.
- [45] L. Ferreira and D. B. Hitchcock, "A comparison of hierarchical methods for clustering functional data," *Communications in Statistics-Simulation and Computation*, vol. 38, no. 9, pp. 1925–1949, 2009.
- [46] V. Estivill-Castro and J. Yang, "Fast and robust general purpose clustering algorithms," in *Pacific Rim International Conference on Artificial Intelligence*. Springer, 2000, pp. 208–218.
- [47] P.-N. Tan et al., *Introduction to data mining*. Pearson Education India, 2006.
- [48] L. Rokach and O. Maimon, "Clustering methods," in *Data mining and knowledge discovery handbook*. Springer, 2005, pp. 321–352.
- [49] S. Aghabozorgi, A. S. Shirkhorshidi, and T. Y. Wah, "Time-series clustering – a decade review," *Information Systems*, vol. 53, pp. 16 – 38, 2015. [Online]. Available: <http://www.sciencedirect.com/science/article/pii/S0306437915000733>
- [50] H. Pirim, B. EkÅşioÅşlu, A. D. Perkins, and ÅGetin YÅjceer, "Clustering of high throughput gene expression data," *Computers & Operations Research*, vol. 39, no. 12, pp. 3046 – 3061, 2012. [Online]. Available: <http://www.sciencedirect.com/science/article/pii/S0305054812000615>
- [51] G. Chicco, R. Napoli, and F. Pigliione, "Comparisons among clustering techniques for electricity customer classification," *IEEE Transactions on Power Systems*, vol. 21, no. 2, pp. 933–940, May 2006.
- [52] A. Goia, C. May, and G. Fusai, "Functional clustering and linear regression for peak load forecasting," *International Journal of Forecasting*, vol. 26, no. 4, pp. 700–711, 2010.
- [53] M. Chaouch, "Clustering-based improvement of nonparametric functional time series forecasting: Application to intra-day household-level load curves," *IEEE Transactions on Smart Grid*, vol. 5, no. 1, pp. 411–419, 2014.
- [54] I. P. Panapakidis, "Clustering based day-ahead and hour-ahead bus load forecasting models," *International Journal of Electrical Power & Energy Systems*, vol. 80, pp. 171–178, 2016.
- [55] V. S. Kodogiannis, M. Amina, and I. Petrounias, "A clustering-based fuzzy wavelet neural network model for short-term load forecasting," *International journal of neural systems*, vol. 23, no. 05, p. 1350024, 2013.
- [56] D. Astolfi, F. Castellani, A. Garinei, and L. Terzi, "Data mining techniques for performance analysis of onshore wind farms," *Applied Energy*, vol. 148, pp. 220 – 233, 2015. [Online]. Available: <http://www.sciencedirect.com/science/article/pii/S0306261915003670>
- [57] R. J. Gil-Garcia, J. M. Badia-Contelles, and A. Pons-Porrata, "A general framework for agglomerative hierarchical clustering algorithms," in *18th International Conference on Pattern Recognition (ICPR'06)*, vol. 2, Aug 2006, pp. 569–572.
- [58] A. Bouguettaya, Q. Yu, X. Liu, X. Zhou, and A. Song, "Efficient agglomerative hierarchical clustering," *Expert Systems with Applications*, vol. 42, no. 5, pp. 2785 – 2797, 2015. [Online]. Available: <http://www.sciencedirect.com/science/article/pii/S0957417414006150>
- [59] F. Murtagh and P. Legendre, "Ward's hierarchical agglomerative clustering method: Which algorithms implement ward's criterion?" *Journal of Classification*, vol. 31, no. 3, pp. 274–295, Oct 2014. [Online]. Available: <https://doi.org/10.1007/s00357-014-9161-z>
- [60] S. Zolhavarieh, S. Aghabozorgi, and Y. Teh, "A review of subsequence time series clustering," *The Scientific World Journal*, pp. 1–19, July 2014.
- [61] D. Berndt and J. Clifford, "Using dynamic time warping to find patterns in time series," vol. 10/16, pp. 359–370, January 1994.
- [62] S. Xihao and Y. Miyanaga, "Dynamic time warping for speech recognition with training part to reduce the computation," in *International Symposium on Signals, Circuits and Systems ISSCS2013*, July 2013, pp. 1–4.
- [63] E. Keogh and C. A. Ratanamahatana, "Exact indexing of dynamic time warping," *Knowledge and Information Systems*, vol. 7, no. 3, pp. 358–386, Mar 2005. [Online]. Available: <https://doi.org/10.1007/s10115-004-0154-9>
- [64] L. Rabiner and B. Juang, *Fundamentals of Speech Recognition*. Prentice-Hall, Upper Saddle River, NJ, USA, 1993.
- [65] T.-C. Fu, "A review on time series data mining," *Engineering Applications of Artificial Intelligence*, vol. 24, no. 1, pp. 164 – 181, 2011. [Online]. Available: <http://www.sciencedirect.com/science/article/pii/S0952197610001727>
- [66] S. Chu, E. Keogh, D. Hart, and M. Pazzani, *Iterative Deepening Dynamic Time Warping for Time Series*, 2002, pp. 195–212.
- [67] C. Cassisi, P. Montalto, M. Aliotta, A. Cannata, and A. Pulvirenti, *Similarity Measures and Dimensionality Reduction Techniques for Time Series Data Mining*, 2012.
- [68] J. Paparrizos and L. Gravano, "k-shape: Efficient and accurate clustering of time series," in *SIGMOD Conference*, 2015.
- [69] T. Giorgino, "Computing and visualizing dynamic time warping alignments in R: The dtw package," *Journal of Statistical Software*, vol. 31, no. 7, pp. 1–24, 2009. [Online]. Available: <http://www.jstatsoft.org/v31/i07/>
- [70] A. Al-Jawad, M. R. Adame, M. Romanovas, M. Hobert, W. Maetzler, M. Traechtler, K. Moeller, and Y. Manoli, "Using multi-dimensional dynamic time warping for tug test instrumentation with inertial sensors," in *2012 IEEE International Conference on Multisensor Fusion and Integration for Intelligent Systems (MFI)*, Sept 2012, pp. 212–218.
- [71] J. Barth, C. Oberndorfer, C. Pasluosta, S. Schulein, H. Gassner, S. Reinfelder, P. Kugler, D. Schuldhuis, J. Winkler, J. Klucken, and B. M. Eskofier, "Stride segmentation during free walk movements using multi-dimensional subsequence dynamic time warping on inertial sensor data," *Sensors*, vol. 15, no. 3, pp. 6419–6440, 2015. [Online]. Available: <http://www.mdpi.com/1424-8220/15/3/6419>
- [72] H. Kaya and S. Gunduz-Oguducu, "Saga: A novel signal alignment method based on genetic algorithm," *Information Sciences*, vol. 228, pp. 113 – 130, 2013. [Online]. Available: <http://www.sciencedirect.com/science/article/pii/S0020025512007955>
- [73] J. Paparrizos and L. Gravano, "k-shape: Efficient and accurate clustering of time series," in *Proceedings of the 2015 ACM SIGMOD International Conference on Management of Data*. ACM, 2015, pp. 1855–1870.
- [74] F. Fahiman, J. C. Bezdek, S. M. Erfani, M. Palaniswami, and C. Leckie, "Fuzzy c-shape: A new algorithm for clustering finite time series waveforms," in *2017 IEEE International Conference on Fuzzy Systems (FUZZ-IEEE)*, July 2017, pp. 1–8.
- [75] "A language and environment for statistical computing," R Foundation for Statistical Computing, Vienna, Austria, 2018. [Online]. Available: <https://www.R-project.com/>
- [76] A. Sarda-Espinosa, "dtwclust: Time series clustering with dynamic time warping distance," R package version 5.5.1., 2018. [Online]. Available: <http://CRAN.R-project.org/package=dtwclust>
- [77] H. Beck and M. Kuhn, "Dynamic data filtering of long-range doppler lidar wind speed measurements," *Remote Sensing*, vol. 9, no. 6, 2017. [Online]. Available: <http://www.mdpi.com/2072-4292/9/6/561>
- [78] H. Akima and A. Gebhardt, "akima: Interpolation of irregularly and regularly spaced data," R package version 0.6-2., 2016. [Online]. Available: <http://CRAN.R-project.org/package=akima>
- [79] Y. Jung, H. Park, D.-Z. Du, and B. L. Drake, "A decision criterion for the optimal number of clusters in hierarchical clustering," *Journal of Global Optimization*, vol. 25, no. 1, pp. 91–111, Jan 2003. [Online]. Available: <https://doi.org/10.1023/A:1021394316112>
- [80] L. Zheng and T. Li, "Semi-supervised hierarchical clustering," in *2011 IEEE 11th International Conference on Data Mining*, Dec 2011, pp. 982–991.

...